

## Performance of the Argo-YBJ detector operated in scaler mode

T. Di Girolamo<sup>a</sup>, G. Di Sciascio<sup>a</sup>, H. H. He<sup>b</sup>, I. James<sup>c</sup>, P. Salvini<sup>c</sup>,  
P. Vallania<sup>d</sup>, Y. G. Wang<sup>b</sup> and F. R. Zhu<sup>b</sup> for the ARGO-YBJ Collaboration

(a) *INFN, Napoli, Italy*

(b) *IHEP-Beijing, China*

(c) *University of Pavia and INFN, Pavia, Italy*

(d) *INAF-IFSI and INFN, Torino, Italy*

Presenter: F. R. Zhu (zhufr@ihep.ac.cn), chn-zhu-F-abs1-og24-oral

The ARGO-YBJ experiment in Tibet has been designed to decrease the energy threshold of typical EAS arrays by exploiting the high altitude location (4300 m a.s.l.) and the full coverage (92 %). The lower energy limit of the detector ( $E > 1$  GeV) is reached by the single particle technique, recording the counting rate at fixed time intervals. At these energies, local (e.g. solar GLE) and cosmological (e.g. GRBs) effects are expected as a significant enhancement of the counting rate over the background. Results on the search of GRBs in coincidence with Swift, HETE and Integral satellites are presented.

### 1. Introduction

A real snapback in the GRB understanding was given by the discovery, due to the Beppo-SAX satellite experiment, of the associated afterglows, and the resultant observations in different wavelengths leading to the distance determination. Nevertheless, there is still a lot of work to be done, and the study of the spectrum high energy tail is an important item. Most GRBs have been observed in the energy range between 20 KeV and 1 MeV. Photons with  $E > 1$  GeV have been detected only for 3 GRBs, by EGRET, that gave in any case the fundamental result of the existence in their flux of photons with energy up to 18 GeV (GRB940217). At these energies the detection from space is hampered by the very low fluxes, requiring large collection areas; from ground the relevant energy range 1 GeV - 1 TeV is partly covered by the Čerenkov telescopes, which last generation has been designed to point at the detected GRB direction in a very short time. The duty cycle is however very low: a wide field detector operating continuously is necessary. The traditional EAS arrays have a threshold energy ( $\sim 50$  TeV) too high, in a region where a signal is strongly absorbed during the propagation due to the  $\gamma$ - $\gamma$  interaction also for moderate distances. A large sensitive area at very high altitude is a very good solution: if operated in scaler mode, i.e. counting the number of particles crossing the detector in a given time interval and searching for an excess in coincidence with a detected signal, it can cover the relevant energy range [1]. Moreover, this detector can be used for GLE studies, usually associated to solar flares, in coincidence with neutron monitors and satellite proton flux monitors. The limitation of this technique is the necessity of working in coincidence, and after the CGRO death no GRB wide field monitor was in operation for years; now, waiting for GLAST, Swift is doing an excellent work, flanked by Integral and HETE.

### 2. The Detector

The experiment is located in Tibet (4300 m a.s.l.) in a huge building (100x110 m<sup>2</sup>) instrumented with a single layer of Resistive Plate Counters (RPC)[2]. At the end of phase 1 (first 2006), 5600 m<sup>2</sup> of active detector are expected; 1900 m<sup>2</sup> are in operation at this moment. The detector has a modular structure, the basic module being a cluster (5.7 x 7.6 m<sup>2</sup>), divided into 12 chambers. Each chamber is read as 10 independent pads of 56 x 62 cm<sup>2</sup>, that are individually acquired and that represent the high granularity pixel of the detector. The carpet is connected to 2 different DAQs, working independently, corresponding to shower mode and scaler

mode operations. In shower mode, for each event the location and timing of each detected particle is recorded, allowing the lateral distribution and arrival direction reconstruction; in scaler mode, only the counting rate of each cluster is measured every 0.5 s, with no informations on the arrival direction and spatial distribution of the detected particles. For each cluster, 4 scalers are used to record the  $\geq 1$ ,  $\geq 2$ ,  $\geq 3$  and  $\geq 4$  rates, with the coincidences defined in a narrow time window (150 ns) and counting rates respectively  $\sim 40$  KHz,  $\sim 2$  KHz,  $\sim 300$  Hz and  $\sim 120$  Hz. The counting rates for a given multiplicity are then obtained using the relation:  $n_i = n_{\geq i} - n_{\geq i+1}$ . Using 4 scalers instead of 1 doesn't improve significantly the sensitivity, but allows us to give an indication of the source spectrum in case of positive detection. For scaler mode operation, the carpet has worked from October 1st, 2004 to March 10th, 2005 with  $667 \text{ m}^2$  sensitive area and 79% efficiency; since March 17th, 2005,  $1750 \text{ m}^2$  are in operation with 88% efficiency (updated June, 2005). The data are continuously checked to give an effective monitoring of the detector performances.

### 3. Effective Area calculation

A detailed MC simulation of both EAS development in the atmosphere and detector response has been carried out for protons and photons of fixed energy ranging from 1 GeV to 1 TeV and zenith angle of  $0^\circ$ ,  $20^\circ$  and  $40^\circ$ . The CORSIKA code 6.18 [3] with QGSJET hadronic interaction model has been used with a full electromagnetic component development down to  $E_{th} = 1 \text{ MeV}$  for both electrons and  $\gamma$ 's. For our purposes it is of crucial importance to correctly simulate the cluster size, i.e. the correspondance between the number of particles hitting the detector and the number of signals generated on the different multiplicity channels. For this reason, the detector simulation results have been compared with an analytical calculation of the multiplicity spread based on the measured cluster size.

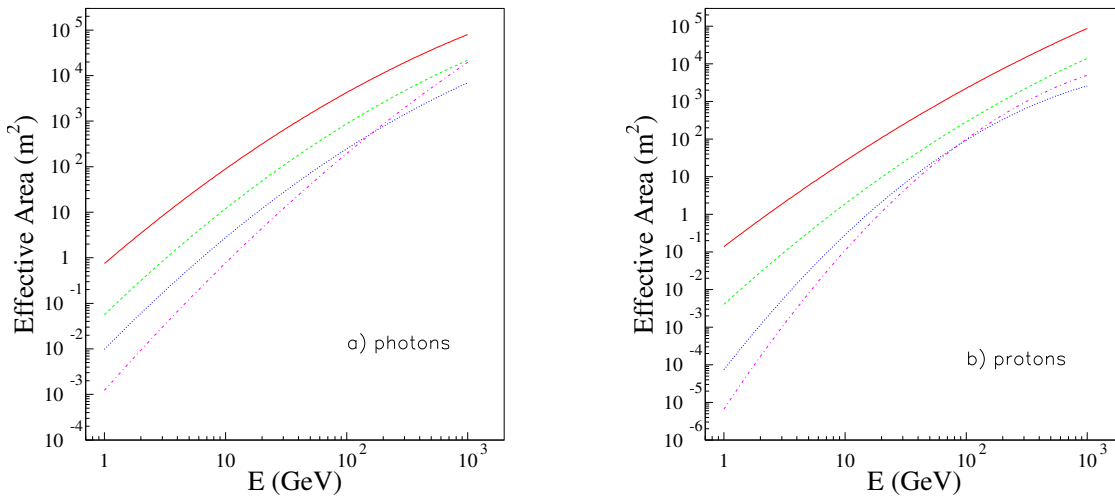


**Figure 1.** Effective area for primary photons (a) and protons (b) with zenith angle  $\theta = 20^\circ$ . The curves refer to the different multiplicity channels:  $n=1$  (continuous),  $n=2$  (dashed),  $n=3$  (dotted) and  $n \geq 4$  (dot-dashed).

Fig. 1 (a,b) shows the effective area for inclined ( $\vartheta = 20^\circ$ ) photons and protons in the 4 multiplicity channels. The values for protons are lower than that for photons at the same energy, increasing the sensitivity of the measurement; moreover the geomagnetic cutoff at YBJ is  $\geq 11 \text{ GV}$  (depending on the arrival direction, both zenith and azimuth), giving an additional bonus to the measurement sensitivity. The effective area is then convoluted with the primary spectrum, with spectral indexes of the differential power law spectra  $\alpha = -2$  for photons (up to  $E_{cut} = 100 \text{ GeV}$ ) and  $\alpha = -2.7$  for protons, taking into account in this case the geomagnetic

**Table 1.** Mode energy and energy range (full width half maximum) for the 4 multiplicity channels, obtained from the convolution between the effective area and the primary spectrum, for  $\gamma$ 's and protons.

Multiplicity	$E_{mode\gamma}$ (GeV)	$E_{range\gamma}$ (GeV)	$E_{modep}$ (GeV)	$E_{rangep}$ (GeV)
1	5	1-83	6.5	1.8-33
2	16	1.2-100	11	2.8-65
3	25	2-100	25	6.4-123
$\geq 4$	100	19-100	52	12.5-240

bending [4]. The mode of the  $\gamma$  distributions increases from  $E = 5$  GeV for singles ( $n=1$ ) to  $E = 100$  GeV for  $n \geq 4$  with a broad distribution, giving the energy region of interest for the detector. Table 1 shows the mode energy and the energy range for the 4 multiplicity channels.

#### 4. Results

Typical fluence upper limits are obtained using the experimental counting rates and a GRB spectrum model. Assuming a power law spectrum up to  $E_{cut} = 100$  GeV with differential spectral index  $\alpha = -2$ , zenith distance  $\vartheta = 20^\circ$ , time duration  $\Delta t = 10$  s and statistical significance  $k = 3$ , the fluence upper limits shown in fig. 2 are obtained for the 4 multiplicity channels. The GRB is assumed close enough to ignore the  $\gamma$  absorption (pair

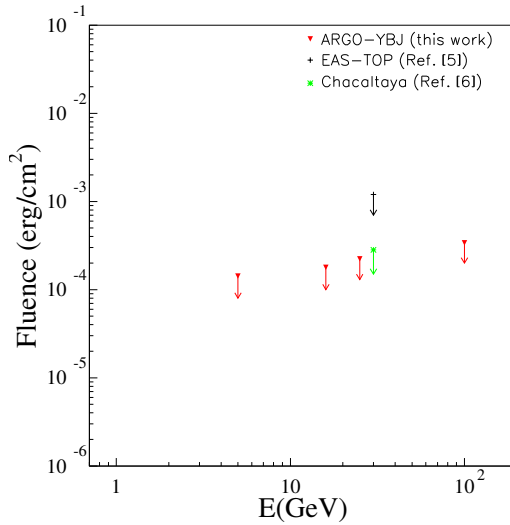


**Figure 2.** Typical Argo-YBJ fluence upper limits for 4 multiplicity channels compared with other experiments (see text).

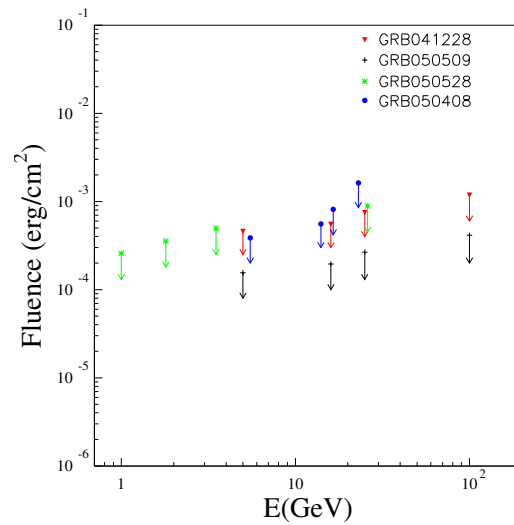


**Figure 3.** Fluence upper limits for 4 GRBs in the Argo-YBJ f.o.v. ( $\theta < 40^\circ$ ). For GRB050408 only, the  $\gamma$  absorption is considered ( $z=1.24$ ).

creation on stellar light photons). In the same plot, some fluence upper limits obtained by other experiments [5],[6] are reported for comparison (scaled with  $\sqrt{\Delta t}$  when necessary). Notice from fig. 2 that if the 4 fluence upper limits are connected by a line, the corresponding differential energy spectrum index is  $\alpha = -1.8$ : a good upper limit can be derived also in case of positive detection in the lower energy channel only ( $n = 1$ ). The GRB search is done in coincidence with Swift, HETE and Integral satellite experiments. The ARGO-YBJ experiment

is linked to the Swift Follow-Up project, allowing a complete GRB analysis in “real time”, while for the other 2 satellites the information is collected on the web [7]. The GRB search was started in correspondence with the first GRB detected by Swift on Dec 17, 2004. Up to now (June 2005) 49 GRBs have been detected, mostly by Swift; 4 of them are in the field of view of Argo ( $\theta < 40^\circ$ ). No signal evidence has been detected; fig. 3 shows the fluence upper limits for these events, using the measured low energy time duration and spectral index (when available, otherwise we assumed  $\alpha = -2$ ),  $E_{max} = 100$  GeV and  $k = 3$ . For GRB050408 the distance is known ( $z = 1.24$ ) and the upper limit is calculated including a simple  $\gamma$  absorption model [8]; for the others  $z = 0$  is assumed. Apart from GRBs, 2 other events have been studied: the SGR 1806-20 flare on Dec 27, 2004, under the ARGO horizon ( $\theta = 99.4^\circ$ ) but perturbing the whole ionosphere, and the solar flare (Class X7) of Jan 20, 2005, connected to a GLE and detected by the Milagro scaler system [9]. No significant coincident excess has been detected so far.

## 5. Conclusions

The search for GRBs chosen with  $\theta < 40^\circ$  in the Argo-YBJ field of view has given no positive result. Nevertheless this simple technique, due to the large sensitive area at very high mountain location, has already shown a good sensitivity, with typical fluence upper limits of  $10^{-3} - 10^{-4}$  erg/cm<sup>2</sup> in the 1-100 GeV energy range. Moreover, using 4 counting channels corresponding to 4 energies well covering the 1-100 GeV region, we can give an indication on the GRB spectrum slope in case of positive detection, and even with a significant excess in the most sensitive multiplicity channel only, a valid maximum spectral index can be derived. We expect to increase the sensitivity by a factor  $\sim 2$  with the detector completion, and to have an equivalent improvement converting the secondary photons of the showers with a 0.5 cm thick layer of lead. A preliminary study [10], applied to the whole Argo-YBJ, has shown that if the GRB spectrum extends at least up to 100 GeV for the most energetic events and their distance doesn't exceed  $z = 2$ , we expect to detect  $\sim 1$  event/year. With these expectations, an accurate check of the detector stability and performances is of crucial importance; a preliminary work can be found in [11].

## 6. Acknowledgements

This work is supported in part by NSFC(10120130794), the Chinese Ministry of Science and Technology, the Chinese Academy of Sciences, the Key Laboratory Astrophysics, IHEP, C.A.S and INFN, Italy

## References

- [1] S. Vernetto, *Astrop. Phys.* 13, 75 (2000).
- [2] Z. Cao et al., "Status of the ARGO-YBJ experiment", these proceedings.
- [3] D. Heck et al., Karlsruhe Report FZKA 6019 (1998).
- [4] T.K. Gaisser and M. Honda, *Ann. Rev. Nucl. Part. Sci.* 52, 153 (2002).
- [5] M. Aglietta et al., *Astroph. Journal* 469, 305 (1996).
- [6] A. Castellina et al., Proc. 27th ICRC, Hamburg (2001), 2735.
- [7] J. Greiner 2005 GRB webpage, <http://www.mpe.mpg.de/jcg/grbgen.html>
- [8] M. H. Salamon and F. W. Stecker, *Astroph. Journal* 493, 547 (1998).
- [9] G. Sinnis, Presentation at the Conference "Towards a Network of Atmospheric Cherenkov Detectors", Palaiseau (France), 27-29 April 2005.
- [10] A. Aloisio et al., *Il Nuovo Cimento* 24C, 4-5, 739 (2001).
- [11] P. Vallania et al., Proc. 28th ICRC, Tsukuba (2003), 2761.